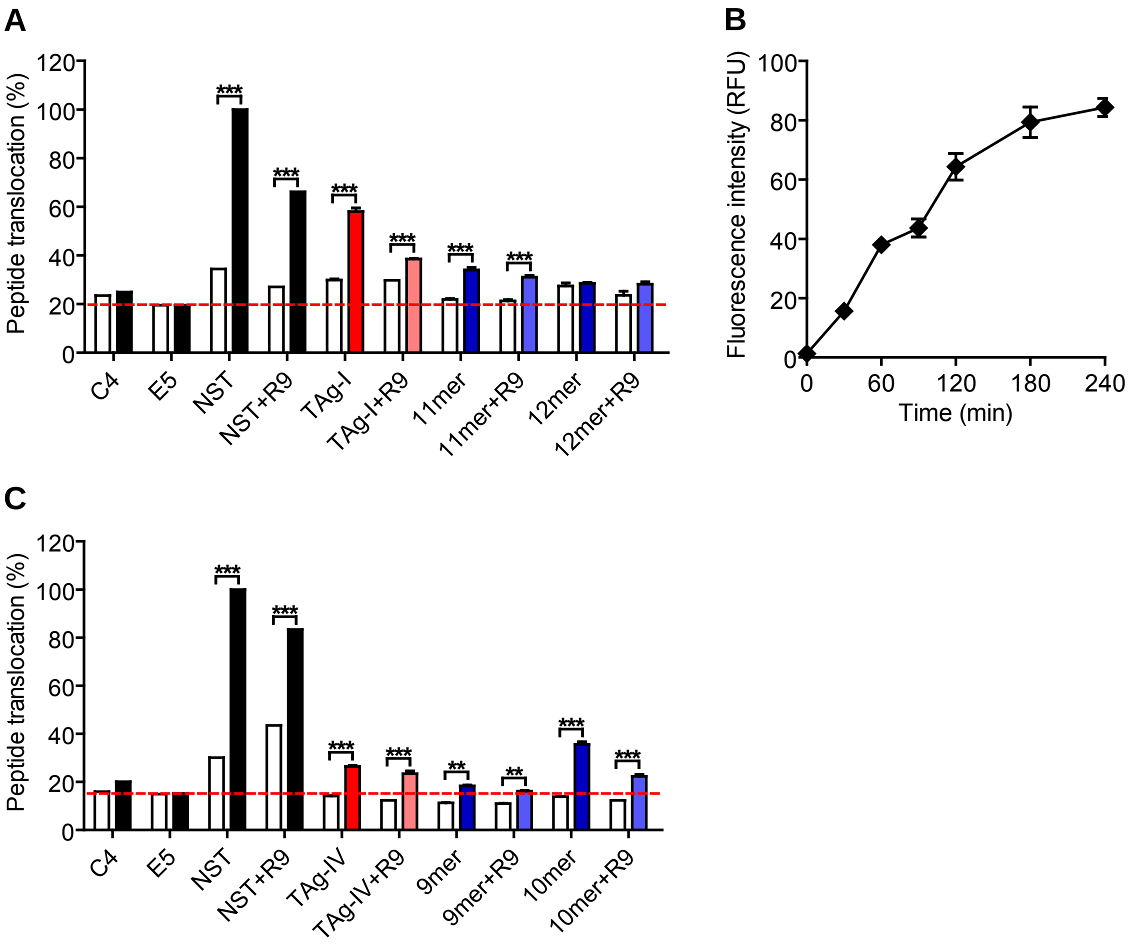


**Figure S1, related to Figure 1**

TAP-dependent peptide translocation in the presence of a high-affinity competitor peptide and activity measurements of recombinant mouse ERAP1 (rmERAP1).

(A) TAP transport was analyzed with 50 µM of each peptide -/+ 50 µM high-affinity competitor peptide (R9) and peptide translocation was calculated. C4: high-affinity peptide devoid of a N-core glycosylation site and labelled with fluorescein, E5: peptide not binding to TAP including a N-core glycosylation site and labelled with fluorescein, NST: reporter peptide including a N-core glycosylation site and labelled with fluorescein. The experimental threshold (red dotted line) was set for E5+ATP (no TAP-binding).
(B) Activity of rmERAP1 was measured by its ability to cleave the fluorogenic peptide substrate H-Leu-AMC. 6 ng rmERAP were incubated with 100 µM H-Leu-AMC at 37°C. The released AMC was measured by a plate reader at excitation/emission wavelengths of 380/460 nm at the indicated time points.
(C) TAP transport was analyzed with 50 µM of each peptide and -/+ 50 µM high-affinity competitor peptide (R9) and peptide translocation was calculated. C4: high-affinity peptide devoid of a N-core glycosylation site and labelled with fluorescein, E5: peptide not binding to TAP including a N-core glycosylation site and labelled with fluorescein, NST: reporter peptide including a N-core glycosylation site and labelled with fluorescein. The experimental threshold (red dotted line) was set for E5+ATP (no TAP-binding).
(A-C) All data are represented as mean ± SD, (A and C) two-way ANOVA.

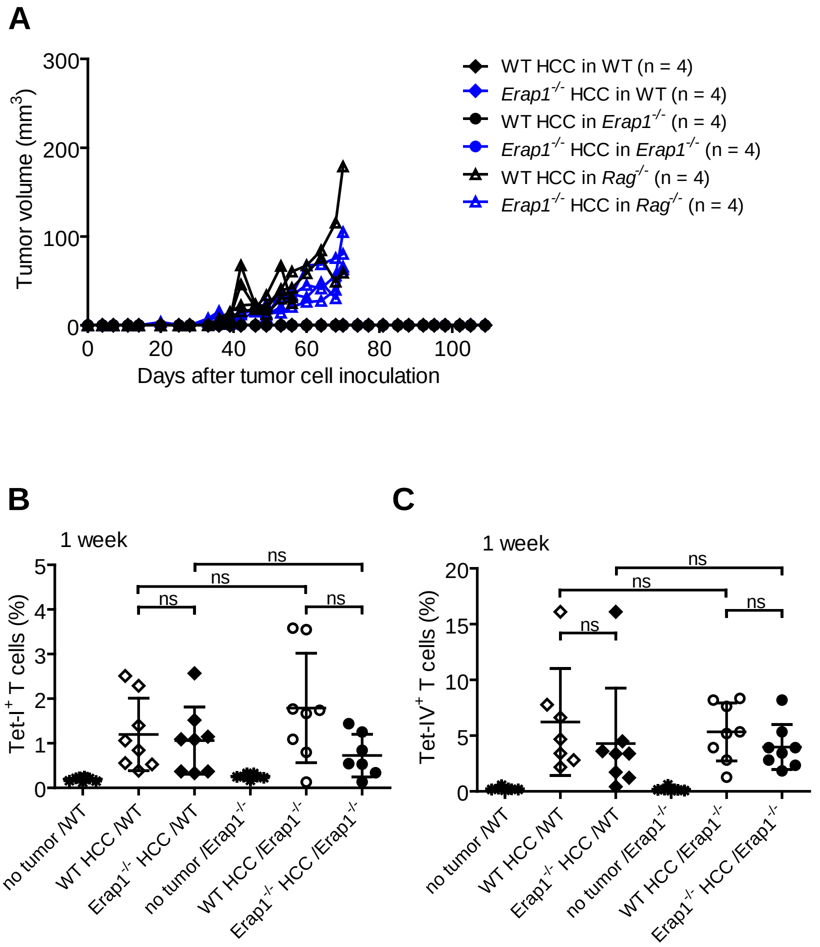


**Figure S2**

WT and *Erap1*$^{-/-}$ HCC are rejected in immune-competent WT and *Erap1*$^{-/-}$ recipients due to priming of TAg-I-specific (Tet-I$^{+}$) and TAg-IV-specific (Tet-IV$^{+}$) CD8$^{+}$ T cells.

(A) 1 x $10^6$ WT or *Erap1*$^{-/-}$ HCC cells were injected s.c. into immune-competent WT (C57BL/6) and *Erap1*$^{-/-}$ recipients (control *Rag*$^{-/-}$ recipients) and the tumor volume was monitored. Shown is a single experiment .
(B) 1 x $10^6$ WT or *Erap1*$^{-/-}$ HCC cells were injected s.c. into immune-competent WT (C57BL/6) and *Erap1*$^{-/-}$ recipients and the percentage of Tet-I$^{+}$ CD8$^{+}$ T cells among polyclonal CD8$^{+}$ $T_E$ cells in peripheral blood was determined one week post ATT.
(C) The experiment was conducted as in (B), and the percentage of Tet-IV$^{+}$ CD8$^{+}$ T cells was determined one week post ATT.
(B and C) Shown is a single experiment, all data are represented as mean ± SD, Kruskal-Wallis test.

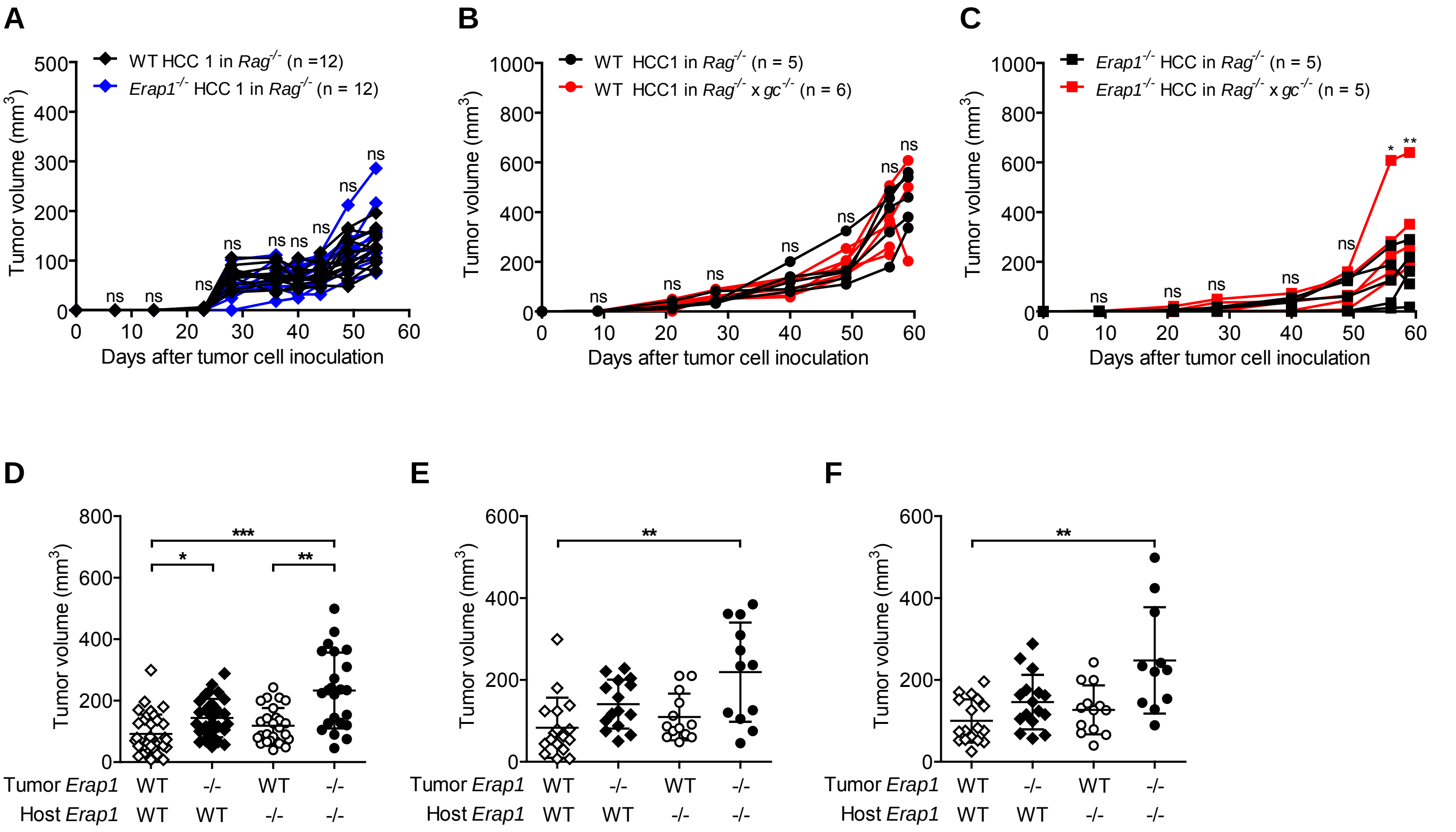


**Figure S3, related to Figures 4 and 5**

Role of NK cells in ERAP1-dependent tumor growth in H2$^{b}$ immune-deficient (*Rag*$^{-/-}$) recipients.

(A) WT and *Erap1*$^{-/-}$ HCC was grown in *Rag*$^{-/-}$ recipients and the tumor volume was monitored. Shown is one of four representative experiments with similar results, two-way ANOVA.
(B) WT HCC was grown in NK cell-competent *Rag*$^{-/-}$ recipients and NK cell-deficient *Rag*$^{-/-}$ x *gc*$^{-/-}$ recipients and the tumor volume was monitored.
(C) *Erap1*$^{-/-}$ HCC was grown in NK cell-competent *Rag*$^{-/-}$ recipients and NK cell-deficient *Rag*$^{-/-}$ x *gc*$^{-/-}$ recipients and the tumor volume was monitored.
(B and C) Data of a single experiment are shown, two-way ANOVA.
(D) Tumor size at the day of ATT shown for all *Rag*$^{-/-}$ H2$^{b}$ recipients (see Figure 4 and Table S3). WT→WT n = 34, *Erap1*$^{-/-}$→WT n = 31, WT→*Erap1*$^{-/-}$ n = 26, *Erap1*$^{-/-}$→*Erap1*$^{-/-}$ n = 23.
(E) Tumor volume of TCR-I T cell-treated H2$^{b}$ *Rag*$^{-/-}$ recipients (see Figure 4C and Table S3B) at the day of ATT. WT→WT n = 17, *Erap1*$^{-/-}$→WT n = 15, WT→*Erap1*$^{-/-}$ n = 13, *Erap1*$^{-/-}$→*Erap1*$^{-/-}$ n = 12.
(F) Tumor volume of TCR-IV T cell-treated H2$^{b}$ *Rag*$^{-/-}$ recipients (see Figure 4D and Table S3C) at the day of ATT. WT→WT n = 17, *Erap1*$^{-/-}$→WT n = 16, WT→*Erap1*$^{-/-}$ n = 13, *Erap1*$^{-/-}$→*Erap1*$^{-/-}$ n = 11.
(D-F) Data of n = 4-5 experiments are represented as mean ± SD, Kruskal-Wallis test, *$p < 0.05$, **$p < 0.01$, ***$p < 0.001$.

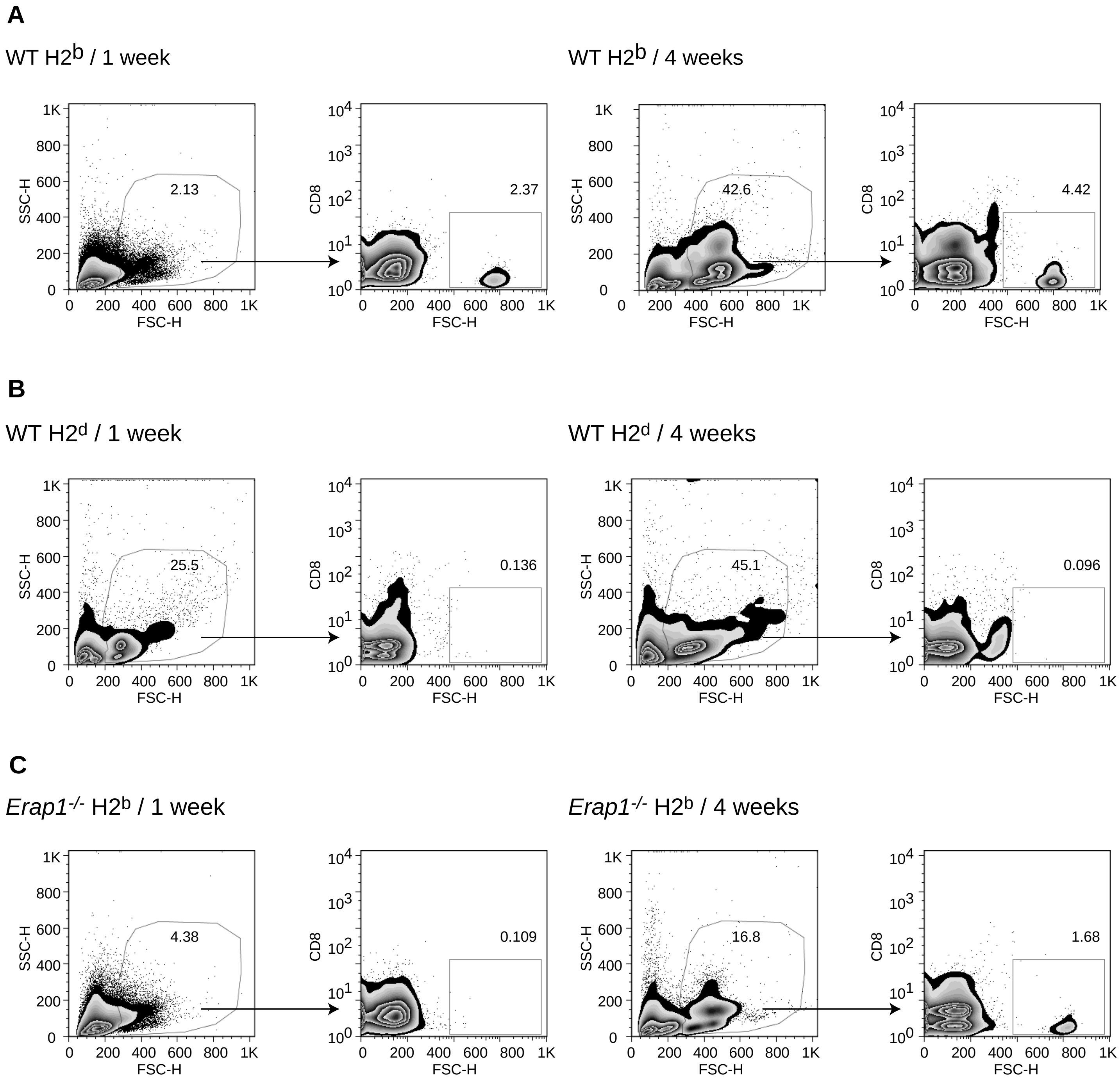


**Figure S4, related to Figure 5**

Gating strategy.

White blood cells were gated on live cells and $CD8^+$ T cells, numbers are % gated cells exemplarily shown for (A) WT x *Rag*$^{-/-}$ recipients (WT $H2^b$), (B) SCID recipients (WT $H2^d$), and (C) *Erap*$^{-/-}$ x *Rag*$^{-/-}$ recipients (*Erap*$^{-/-}$ $H2^b$) 1 week and 4 weeks after ATT.

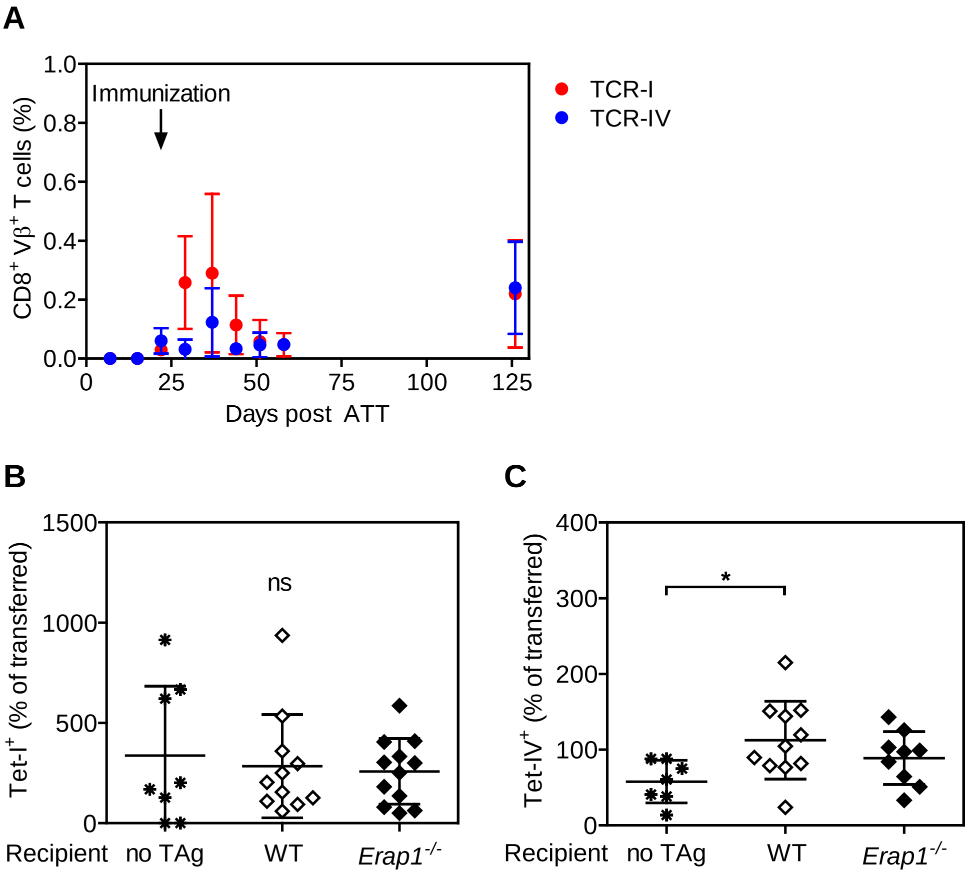


**Figure S5, related to Figure 5**

Antigen-dependent expansion of TCR-I and TCR-IV T cells.

(A) 1 x $10^6$ TCR-I T cells and 1 x $10^6$ TCR-IV T cells were co-tranferred into immune-deficient *Rag*$^{-/-}$ mice (n = 3 mice per group). % $CD8^+$ $Vß7^+$ TCR-I T cells and $CD8^+$ $Vß9^+$ TCR-IV T cells were measured in at different time points after ATT in peripheral blood. Mice were immunized with irradiated $TAg^+$ 16.113 tumor cells on day 22 post ATT. Data are represented as mean ± SD.
(B) TCR-I (Tet-$I^+$) $CD8^+$ cells among polyclonal $CD8^+$ $T_E$ cells in peripheral blood on day 7 post ATT. No Tag n = 8, WT n = 11, *Erap1*$^{-/-}$ n = 12 mice.
(C) TCR-IV (Tet-$IV^+$) $CD8^+$ cells among polyclonal $CD8^+$ $T_E$ cells in peripheral blood on day 7 post ATT. No Tag n = 7, WT n = 11, *Erap1*$^{-/-}$ n = 9 mice.
(B, C) Percentage was calculated according to % of Tet-$I^+$ (1.74) and Tet-$IV^+$ (17.5) $CD8^+$ T cells among 1 x $10^6$ polyclonal $CD8^+$ $T_E$ cells transferred on day 0. Data are represented as mean ± SD, Kruskal-Wallis test, *$p < 0.05$.

**A**

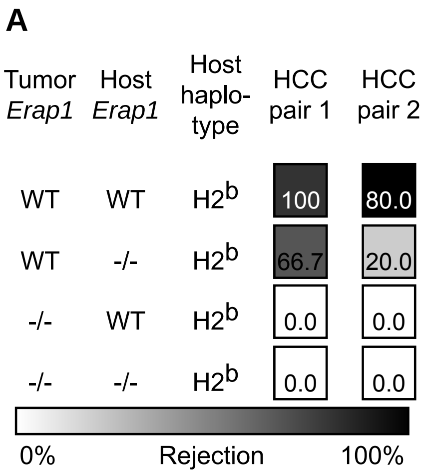


**B**

| Tumor *Erap1* | WT | WT | *Erap1*$^{-/-}$ | *Erap1*$^{-/-}$ |
|---|---|---|---|---|
| Host *Erap1* | WT | *Erap1*$^{-/-}$ | WT | *Erap1*$^{-/-}$ |
| Host haplotype | H2$^b$ | H2$^b$ | H2$^b$ | H2$^b$ |
| HCC pair 1 | 6/6 (100) | 2/3 (66.7) | 0/5 (0.0) | 0/3 (0.0) |
| HCC pair 2 | 8/10 (80.0) | 2/10 (20.0) | 0/4 (0.0) | 0.3 (0.0) |
| Rejection | 14/16 (87.5) | 4/13 (30.8) | 0/9 (0.0) | 0/6 (0.0) |

**C**

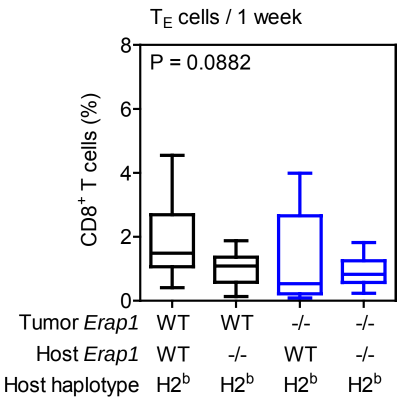


**D**

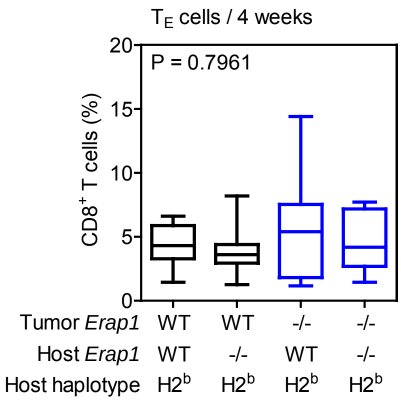


**Figure S6, related to Figure 6**

TAg$^+$ HCC rejection through polyclonal CD8$^+$ $T_E$ cells and expansion of polyclonal CD8$^+$ $T_E$ cells after ATT.

(A) Graphical representation of rejection of WT and *Erap1*$^{-/-}$ TAg$^+$ HCC by polyclonal CD8$^+$ $T_E$ cells in WT and *Erap1*$^{-/-}$ H2b$^+$ recipients.
(B) Numerical summary of the tumor rejection experiments using polyclonal CD8+ $T_E$ cells. Data represent the number of analyzed mice of n = 2 - 6 experiments per HCC pair / group, % rejection are parenthesized.
(C) FACS analysis of CD8+ $T_E$ cell expansion 1 week after ATT. WT→WT n = 10 mice, *Erap1*$^{-/-}$→WT n = 14 mice, WT→*Erap1*$^{-/-}$ n = 8 mice, *Erap1*$^{-/-}$→*Erap1-/-* n = 10 mice.
(D) FACS analysis of CD8+ $T_E$ cell expansion 4 weeks after ATT. WT→WT n = 10 mice, *Erap1*$^{-/-}$→WT n = 14 mice, WT→*Erap1*$^{-/-}$ n = 8 mice, *Erap1*$^{-/-}$→*Erap1*$^{-/-}$ n = 10 mice.
(C and D) All data are represented as mean ± SD, Kruskal-Wallis test.

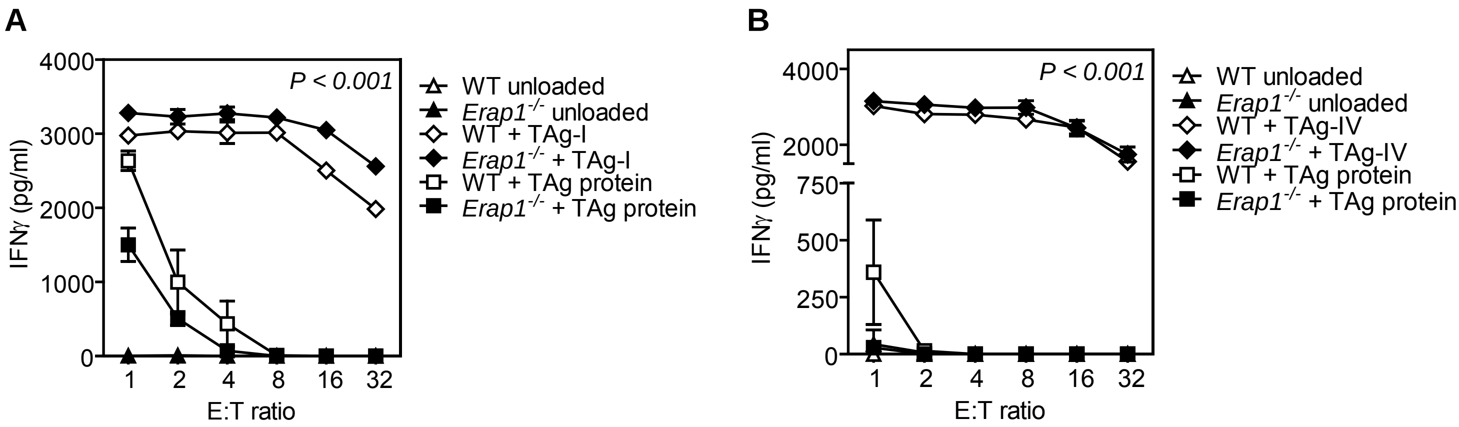


**Figure S7**

Analysis of ERAP1-dependent cross-presentation of TAg-I and TAg-IV by bone marrow-derived dendritic cells (BMDCs).

(A) Cross-presentation of TAg-I processed from full-length TAg protein was analyzed in $CD11c^+$ WT or *Erap1*$^{-/-}$ GM-CSF-differentiated BMDCs. After 7 days of co-culture with 20 ng/ml GM-CSF, BMDCs were loaded with 0.1 μM TAg-I or 30 ng purified TAg protein for 2 hours at 37°C, and were co-cultured with TCR-I T cells for 18 hours. Release of IFNγ was measured by ELISA.
(B) Cross-presentation of TAg-IV processed from full-length TAg protein was analyzed in $CD11c^+$ WT or *Erap1*$^{-/-}$ GM-CSF-differentiated BMDCs. The experiment was performed as described for (A), but BMDCs were co-cultured with TCR-IV T cells.
(A and B) Shown is one of two independent experiments with similar results. All data are represented as mean ± SD, two-way ANOVA.